Spatio-temporal Variation of Building Morphology in Indian Cities from 2018 to 2023

Nishchaya Kumar Mishra[1,a], Sameer Patel[1, 2, 3,b], Sushobhan Sen[1,3,c]

[1]Department of Civil Engineering, [2]Department of Chemical Engineering, [3]Kiran C. Patel Centre of Sustainable Development, Indian Institute of Technology Gandhinagar, Palaj, Gandhinagar, Gujarat 382355, India
[a]nishchayamishra@iitgn.ac.in, [b]sameer.patel@iitgn.ac.in, [c]sushobhan.sen@iitgn.ac.in

Abstract

By 2050, more than two-thirds of the world's population is estimated to reside in urban areas, leading to a rapid increase in the consumption of resources in cities. Depending on factors such as urban sprawl and building morphology, this can lead to several adverse effects on the environment and public health, such as energy consumption and the Urban Heat Island effect. Rapidly developing countries like India have a great degree of unplanned expansion and building construction, with significant growth in urban infrastructure expected in the next 15 years. Therefore, it is critical to understand the evolution of building morphology in the process of urban development. This study examines the evolution of building morphology in 11 major Indian cities over two years: 2018 and 2023. Remote sensing data was coupled with a deep learning model, Simultaneous building Height And FootprinT extraction from Sentinel imagery (SHAFTS), for quantifying building height and footprint in these cities. A variability index was defined to quantify the spatial variability, demonstrating that height variabilities are more significant than footprint for 2018 and 2023. Chandigarh (0.0557 km^{-1}) and Mumbai (0.0351 km^{-1}) have the highest and the lowest footprint variability, while Bangalore (0.0739 km^{-1}) and Mumbai (0.0441 km^{-1}) have the highest and lowest height variability in 2023. Barring a few cities, the footprint variability decreased from 2018 to 2023, indicating that the newer buildings have similar footprints to existing ones. Contrarily, the increased height variability indicates height differences between the older and newly constructed buildings.

Keywords
Urban planning, Building morphology, Machine learning, Remote sensing, Sustainable development

1. Introduction

Currently, more than half of the global population resides in urban areas, which is projected to increase to 68% by 2050 [1]. To accommodate this growth, cities worldwide have expanded, and newer urban settlements have grown to meet the increased demand owing to economic and societal development, and to improve the quality of life [2]. The primary determinant to measure the increase in urban settlements is buildings, which have grown by over 30% in the past decade [3]. These urban settlements cover a small fraction of the Earth's surface; however, their impact on humans and the urban climate is significant. For example, buildings consume more than one-third of the global energy demand [4], which is only increasing with time. Simultaneously, they account for over one-third of energy and process-related carbon emissions [3], thus adding to climate change and creating a causal loop between building design and operation, and climate change [5,6]. Moreover, the indoor environments in buildings present an interdependent complex system between pollutant exposure, comfort, and energy consumption, affecting occupants' health and well-being [7–9]. Besides energy consumption, carbon emissions, and occupants' health, these urban forms represent a country's social, cultural, and economic divide [10–13].

Recent studies have correlated the shape and structure of buildings with differential living spaces in urban and rural areas [10], urban heat island effects [14–17], and the mental and physical wellness of citizens [18,19]. The shape and height of buildings also affect their energy consumption profile [20,21] and govern the airflow pattern in the neighbourhood. The airflow pattern affects the fate of pollutants and thereby directly impacts public health [22–25]. Hong et al., [26] studied the effect of urban two-dimensional (coverage or density) and three-dimensional (building height) morphology on ozone concentration in 68 cities. The study reported the highest urban ozone concentration in low-rise high-density cities, and the analysis indicated that urban morphology was a significant factor influencing ozone concentration [26]. Moreover, taller buildings cast a shadow on their surroundings, affecting

various applications such as solar energy integration and differential heating and cooling effects, further affecting resource consumption and public health [27–29]. In summary, buildings significantly impact human health and the environment and play a major role in realizing multiple Sustainable Development Goals (SDGs). Therefore, studying the existing and expected future urban forms, especially building morphology, is essential to ensure a holistic and sustainable approach to urban planning and management for promoting energy equity, human and environmental health, and achieving SDGs.

Past research has developed machine learning and image processing techniques integrated with remote sensing to predict building height and footprint at varying spatial resolutions [30–36]. For example, Frantz et al. [37] combined Sentinel-1A/B and Sentinel-2A/B time series data to map building heights for all of Germany on a 10m grid. On the other hand, Li et al. [30] developed a deep-learning-based model to simultaneously extract building height and footprint at four resolutions (100, 250, 500, and 1000m). These deep-learning models can be leveraged to study the heterogeneity in building height and footprint within a city that is critical to addressing multiple urban planning and management challenges, such as devising urban heat island mitigation strategies, controlling pollutant transport, optimizing waste collection and management, integrating renewable energy resources, and benchmarking energy and resource consumption. Moreover, developing countries like India have a greater degree of unplanned expansion and building construction [38]. India is rapidly urbanizing, with the construction sector expected to grow to $1 trillion in the next 15 years [39]. This substantial growth in the building stock will increase resource consumption, carbon emissions, and environmental impacts while leading to restricted airflow and heating of neighborhoods. Therefore, it is critical to study the urban morphology of Indian cities to understand the spatial and temporal patterns and variations in building height and footprint.

The growth of urban settlements by analyzing land use and land cover changes over time has been widely studied [40–46]. However, changes in building height and footprint within a city have received limited attention, and a literature review did not reveal any studies for Indian cities. This study analyzes

the spatial and temporal changes in building height and footprint in 11 Indian cities. A deep-learning model developed by Li et al. [30], called Simultaneous building Height And FootprinT extraction from Sentinel imagery (SHAFTS), has been integrated with remote-sensing data for multiple cities over two years (2018 and 2023) to examine the patterns in building footprint and height and their evolution between the two years. A novel framework for identifying the variability of these two urban morphology parameters, called the variability index, was developed. Firstly, the spatial changes in the variability index have been analyzed, representing the degree of uniformity in height and footprint within a city. Secondly, the temporal changes between 2018 and 2023 were analyzed to illustrate how these parameters have changed over time. The results presented in this study can aid in policy-making for Indian cities to ensure sustainable and healthy urban environments and design strategies to mitigate air quality challenges, urban heat island effects, and resource consumption.

2. Data and Methods

2.1 Study Area

Eleven major cities in India have been selected in this study based on population, industrialization level, and regional connectivity. These are shown as a map in Fig. 1. For the present study, each city was assumed to occupy an area of approximately 500 km^2. This bound has been selected to represent the existing urban forms in any city. While the chosen bounds may not cover the entire city, it is assumed that the variations across any city are similar to what has been captured within the bounds of the respective city. Challenges, such as computational and data needs, must be addressed if the complete area of all cities has to be considered for analysis. The geographical bounds of the cities, to capture the area mentioned earlier, were selected as shown in Table 1.

Table 1. Cities investigated in this study and their geographical bounds

City Name	Geographical Bounds			
	Longitude Minimum (East)	**Latitude Minimum (North)**	**Longitude Maximum (East)**	**Latitude Maximum (North)**
Ahmedabad	72.50°	22.95°	72.70°	23.15°

Bangalore	77.55°	12.90°	77.75°	13.10°
Chandigarh	76.65°	30.62°	76.85°	30.78°
Chennai	80.03°	12.94°	80.26°	13.15°
Delhi	77.00°	28.50°	77.20°	28.80°
Hyderabad	78.30°	17.35°	78.60°	17.55°
Jaipur	75.70°	26.80°	75.90°	27.00°
Kolkata	88.23°	22.44°	88.45°	22.64°
Mumbai	72.82°	19.00°	72.95°	19.30°
Pune	73.75°	18.42°	73.95°	18.64°
Surat	72.75°	21.05°	72.94°	21.27°

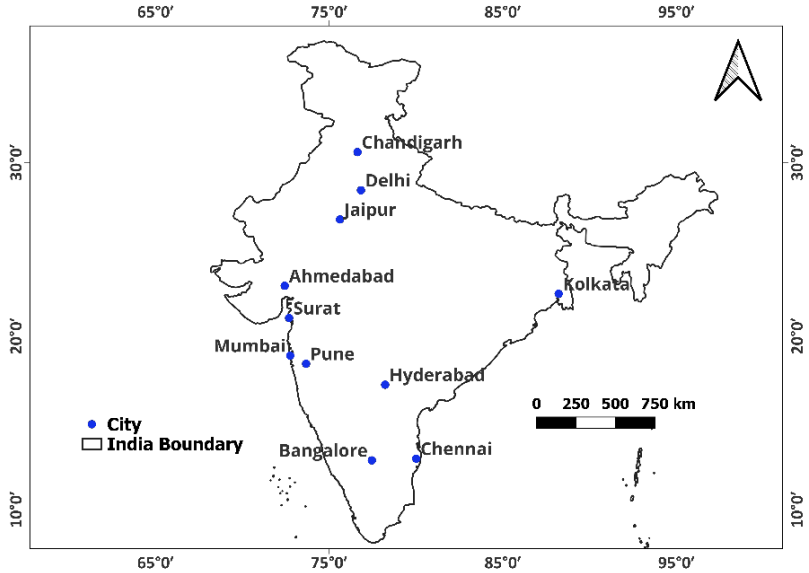

Figure 1. Map of India with the location of eleven cities selected for study in this work.

2.2 Research Framework and Input Remote Sensing Data

Unlike several cities in the Global North, the 11 Indian cities selected do not have a comprehensive building morphology database. This is typical of cities in the Global South. Therefore, the present study extracted and analyzed building morphology for these cities using the workflow shown in Fig. 2. The investigation has been divided into three levels.

In Level 0, for each of the 11 cities identified above, the following remote sensing data were obtained for the years 2018 and 2023 using Google Earth Engine [47]:

(i) 10m VV and VH polarizations of ground range detected level-1 products of Sentinel-1 images.

(ii) 10m red, green, blue, and the near-infrared band of level-2A products of Sentinel-2 images.

(iii) 30m digital elevation model (DEM) data from the SRTM V3 product.

Next, the urban morphology in terms of average building height (in metres) and footprint per pixel (in m^2/m^2), at a resolution of 100 m, was estimated using the deep-learning-based model SHAFTS developed by Li et al. [30]. The model has been previously validated and used for 46 cities across the world, but the current work is the first application of SHAFTS for India.

In Level 1, the output maps from Level 0 are transformed into their corresponding Fourier domain (i.e., wavenumber domain) and are shifted by different ground distances in the spatial domain. Finally, in Level 2, a correlation analysis is performed between the original and shifted images to identify the variability in the urban morphology in each city. Levels 0-2 are expressed in greater detail in the following sections.

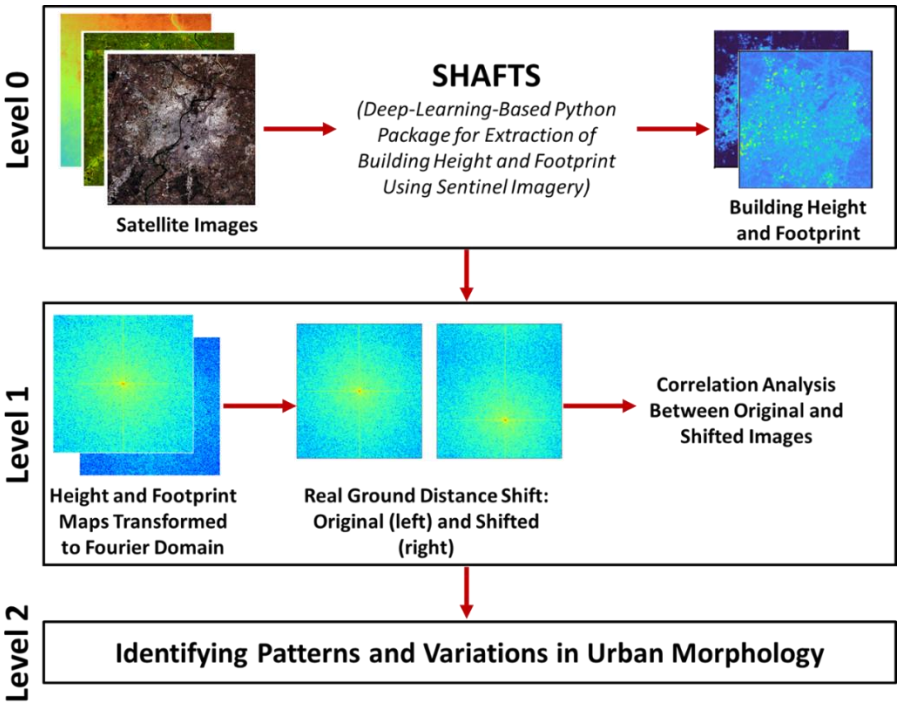

Figure 2. Workflow of this study.

2.3 Overview of the SHAFTS Model and Prediction of Building Height and Footprint

The SHAFTS model, developed by Li et al. [30] in 2023, provides a trained and validated model for predicting average building height and footprint at multiple spatial resolutions (100 m, 250 m, 500 m,

and 1000 m) for any given city. It is available as a package written in the Python programming language [48]. In this model, Li et al. proposed a multi-task deep-learning (MTDL) model to automatically learn feature representation shared by building height and footprint. The DEM information has been integrated into the developed models to inform them about the terrain-induced effects on the backscattering displayed by the Sentinel images. The study showed that the developed MTDL model had higher accuracy in building height and footprint predictions than conventional machine-learning-based models such as random forest regression, support vector regression, and XGBoostR. The pre-trained model at 100m resolution has been used in this study as it offers the highest resolution for analyzing the unplanned building layouts of the 11 Indian cities.

2.4 Image Representation in Wave Number (Fourier) Domain

The predicted building height and footprint map for the 11 cities obtained from the SHAFTS model are represented in the spatial domain, in which average building height and footprint are represented per pixel in space. In order to quantify their variability within each city, the differences in building height and footprint at different locations within the city need to be evaluated. A common method used in the literature for this is the method of autocorrelation, in which an image is shifted by a fixed number of pixels (distance) and the correlation between the original and shifted pixels is calculated (as shown in Eq. (1)).

$$corr(x,y) = \frac{\sum_{i=1}^{N}(x_i - \bar{x})(y_i - \bar{y})}{\sqrt{\sum_{i=1}^{N}(x_i - \bar{x})^2}\sqrt{\sum_{i=1}^{N}(y_i - \bar{y})^2}}$$

Eq. (1)

where x and y are the sample points, N is the sample size, and $\bar{x}$ and $\bar{y}$ are the sample means.

If the variability in the image is low, then the correlation coefficient is expected to be close to unity; likewise, if the variability is high, the correlation coefficient is expected to be close to zero. However,

a significant downside to this approach is that it can only be used to evaluate local variability, i.e., the variability around only a handful of pixels. It cannot be used to assess the overall variability of building morphology in the entire city. An alternative method was adopted to overcome this shortcoming of autocorrelation in the spatial domain. The images in the spatial domain were converted to the wavenumber domain (also called the Fourier domain) using a Discrete Fourier Transform (DFT) using Eq. (2) for an $N \times N$ image below.

$$F(K,L) = \sum_{i=0}^{N-1}\sum_{j=0}^{N-1} f(i,j)e^{-i2\pi(\frac{K_i}{N}+\frac{L_j}{N})}$$

Eq. (2)

where *f(i, j)* is the image in the spatial domain, and the exponential term is the basis function corresponding to each point *F(K, L)* in the Fourier domain, where K and L are the wavenumbers in each direction. As the traditional FT algorithm is computationally expensive, a Fast Fourier Transform (FFT) developed by Cooley and Tukey [49] has been used in this study.

DFT produces a complex number-valued output image, which can be displayed with two images, either with the real and imaginary parts or with magnitude and phase [50,51]. Each point in the Fourier domain image represents the relative spectral power of a particular wavenumber in the image. The wavenumber represents the spatial variability in the image (building height and footprint, in this case): larger wavenumbers indicate relatively uniform images, while smaller wavenumbers indicate more variability. Thus, the building morphology data, when transformed into the Fourier domain, provides a snapshot of the variability of morphology in each city as a whole.

2.5 The variability index

For the analysis conducted in this work, true wavenumbers were used instead of the indices of those frequencies. Therefore, the zero-wavenumber component is shifted to the center of the spectrum, and

the coefficients are reordered. Moreover, the intensity values were larger, so a logarithmic transformation was applied to enhance the contrast in the representations. The height and footprint map representations of different cities in the Fourier domain have the lowest frequency at the center, and higher frequencies are located away from the center.

As the images after FT represent the variability in each city as a whole, autocorrelation could be performed on the transformed images to study the spatial variations in building height and footprint. Unlike autocorrelation on the images themselves, this approach captures the variability of the city as a whole. The FT images were shifted for multiple combinations of vertical and horizontal ground distances, and correlations were estimated between the original and shifted images. In this case, for a given shift, a high correlation coefficient represents a relatively uniform city, whereas a low coefficient represents one with a higher variability. Moreover, as the shift distance increases, the correlation coefficient for a relatively uniform city is expected to decrease slowly, whereas a city with high variability would see a significant decrease in the coefficient as the shift increases. Therefore, the present study developed a variability index, which is the rate of change of the correlation coefficient between the FT images and the shifted FT images as the shift increases (estimated as shown in Eq. (3)). This index was used to compare the spatial variability in building height and footprint in the 11 selected cities, while the change in the index between 2018 and 2023 was used to assess the temporal changes in the cities.

$$\Delta corr = \frac{corr_{FT\ images_{zero\ shift}} - corr_{FT\ images_x}}{\Delta x}$$

Eq. (3)

where, $corr_{FT\ images_{zero\ shift}}$, and $corr_{FT\ images_x}$ are the correlation coefficients between FT images and shifted images at zero shift and shift of x km, respectively. Δx is the step size in the shift distance, which is 1 km in this study.

3. Results and Discussion

3.1 Building Footprint and Height Map for Selected Indian Cities

The building footprint and height maps obtained from the SHAFTS model are shown in Fig. 3 and Fig. 4, respectively, for each of the 11 cities. The footprint (m^2/m^2) is the ratio of the building area in a pixel and the total area within that pixel. Therefore, for all cities, the footprint varies between zero and one, where zero means no buildings were present in the pixel and one implies that buildings cover the entire pixel. It can be seen that the footprint maps have also identified urban features such as rivers, lakes, roads, and zero-building areas like parks. For example, the rivers have been delineated accurately for Ahmedabad (Fig. 3A), Kolkata (Fig. 3H), Pune (Fig. 3J), Surat (Fig. 3K), and the lakes in Bangalore have been identified with zero building footprint (Fig. 3B). The high-density urban areas distributed in different parts of the cities can also be observed.

Similarly, the building height maps (Fig. 4) obtained from the SHAFTS model represent the average building height in any image pixel in meters. However, urban morphology delineation needs to be done based on aggregated information from both building footprint and height maps, as some pixels might be misclassified. For example, the river in Kolkata has been accurately identified in the footprint map (Fig. 3), but it has been misclassified in the height map (Fig. 4). Also, the footprint and height predictions for Chennai show some unusual behaviour for 2018, that has been translated to these maps from the satellite data used as inputs to the SHAFTS model for predictions. Nevertheless, barring a few instances of misclassification, the overall building morphology information seemed satisfactory.

3.2 Fourier Domain Images

The magnitude spectrum of the wavenumber (Fourier) domain representations of building footprint and height maps are shown in Fig. 5 and Fig. 6, respectively. The Fourier domain images show a mixture of high and low-wavenumber components with varying magnitudes. For both height and footprint representations in the Fourier domain, the low-wavenumber components at the center have

the highest magnitude, especially for the footprint map, indicating a certain degree of uniformity. Nonetheless, the high-wavenumber components also have a significant spectral power, indicating a fair amount of variability in each city as well. The comparison of height and footprint representations suggests that the change in height is more significant in all cities compared to the footprint of buildings, which is discussed in detail in the upcoming sections.

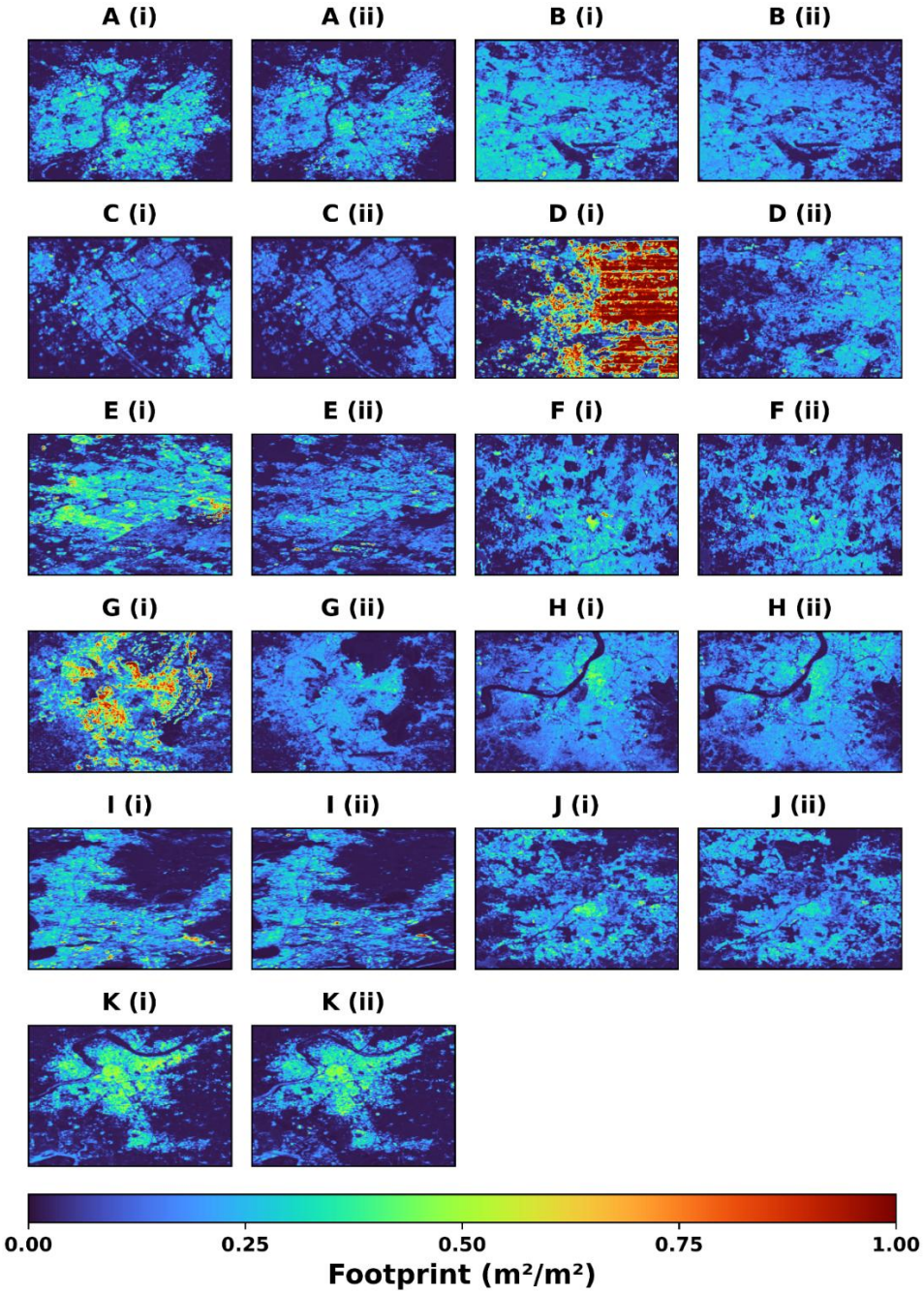

Figure 3. Building footprint maps for 11 Indian cities: (A) Ahmedabad, (B) Bangalore, (C) Chandigarh, (D) Chennai, (E) Delhi, (F) Hyderabad, (G) Jaipur, (H) Kolkata, (I) Mumbai, (J) Pune, and (K) Surat for (i) 2018 and (ii) 2023.

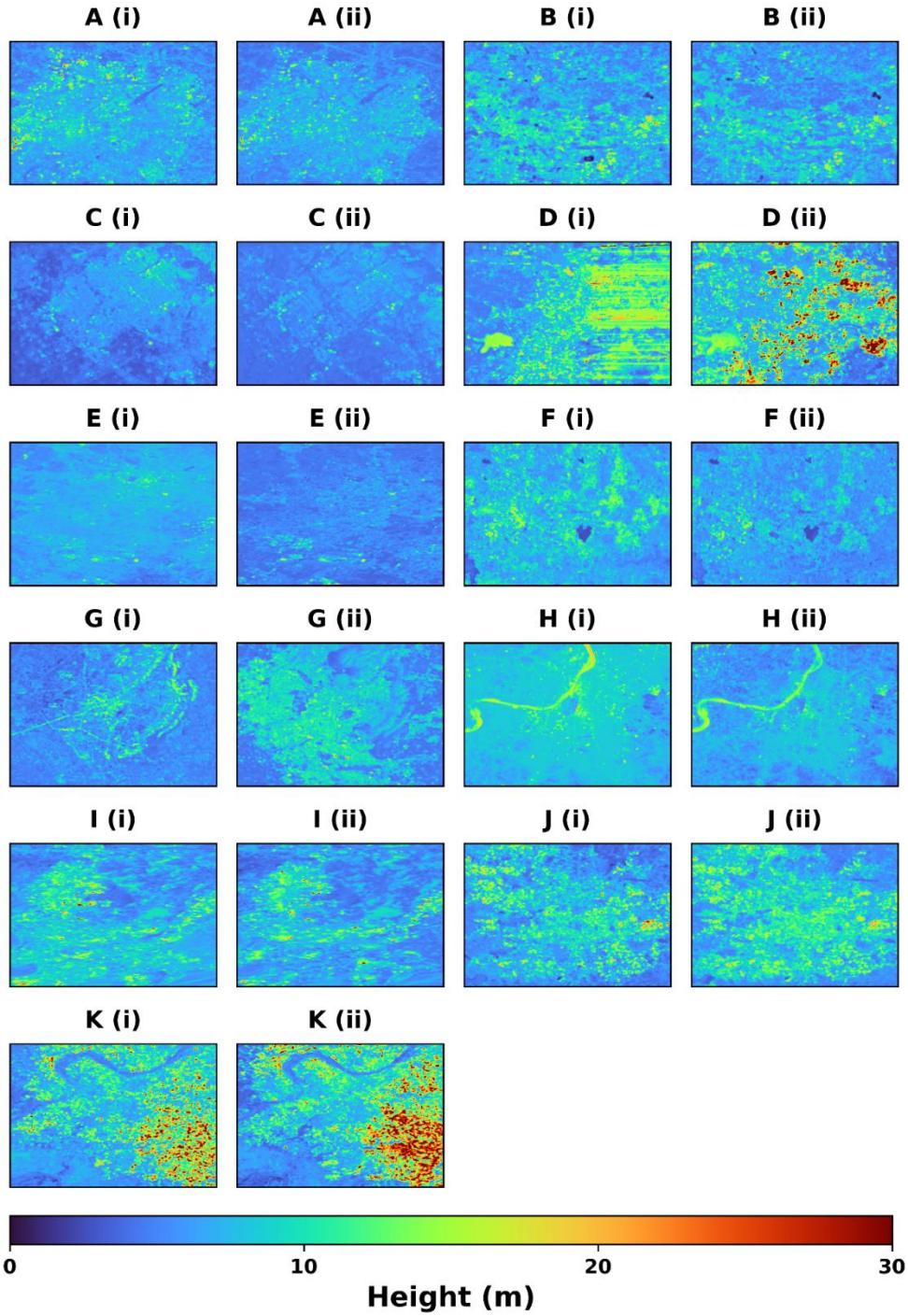

Figure 4. Building height maps for 11 Indian cities: (A) Ahmedabad, (B) Bangalore, (C) Chandigarh, (D) Chennai, (E) Delhi, (F) Hyderabad, (G) Jaipur, (H) Kolkata, (I) Mumbai, (J) Pune, and (K) Surat for (i) 2018 and (ii) 2023.

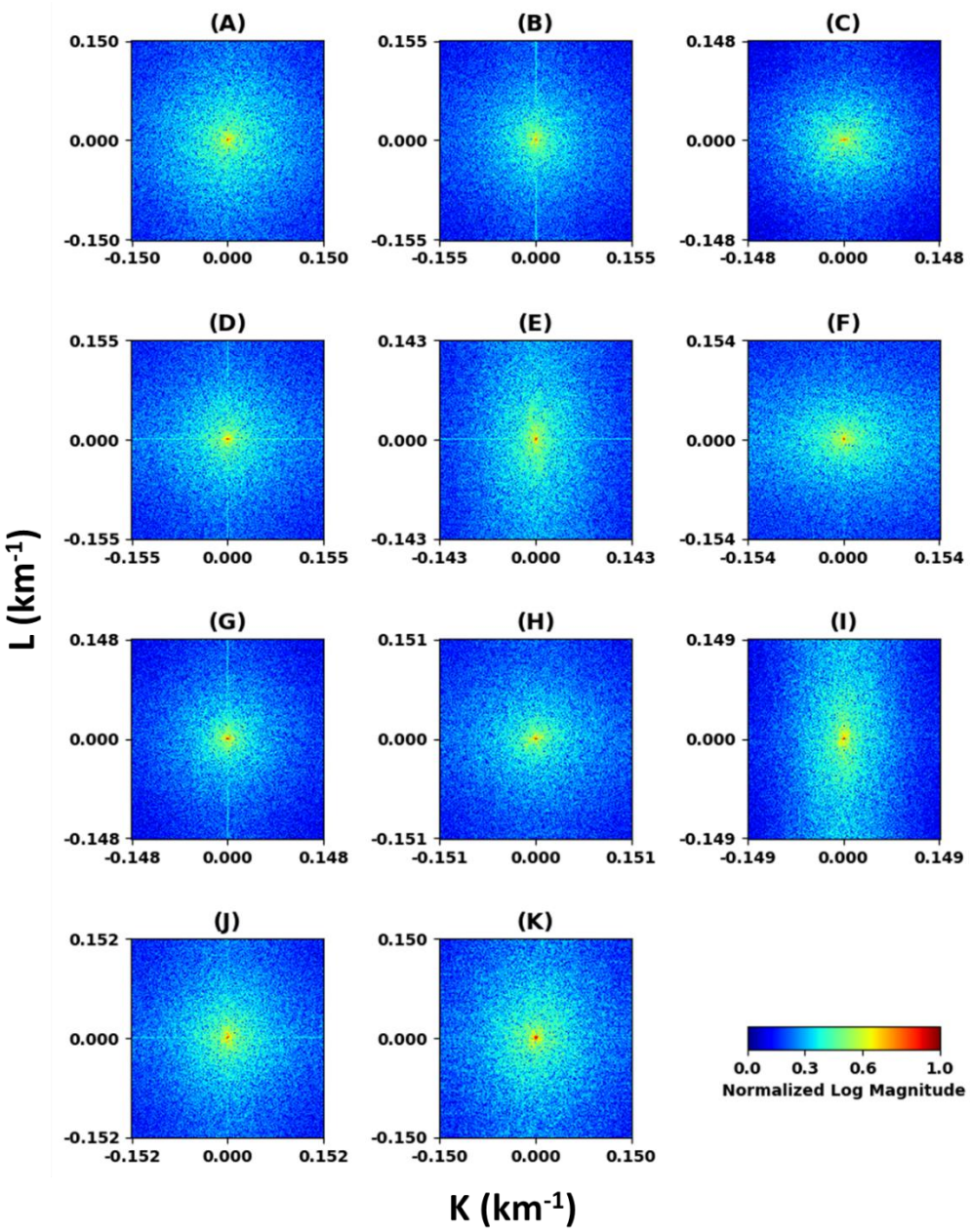

Figure 5. Fourier domain representation of footprint maps for selected Indian cities: (A) Ahmedabad, (B) Bangalore, (C) Chandigarh, (D) Chennai, (E) Delhi, (F) Hyderabad, (G) Jaipur, (H) Kolkata, (I) Mumbai, (J) Pune, and (K) Surat.

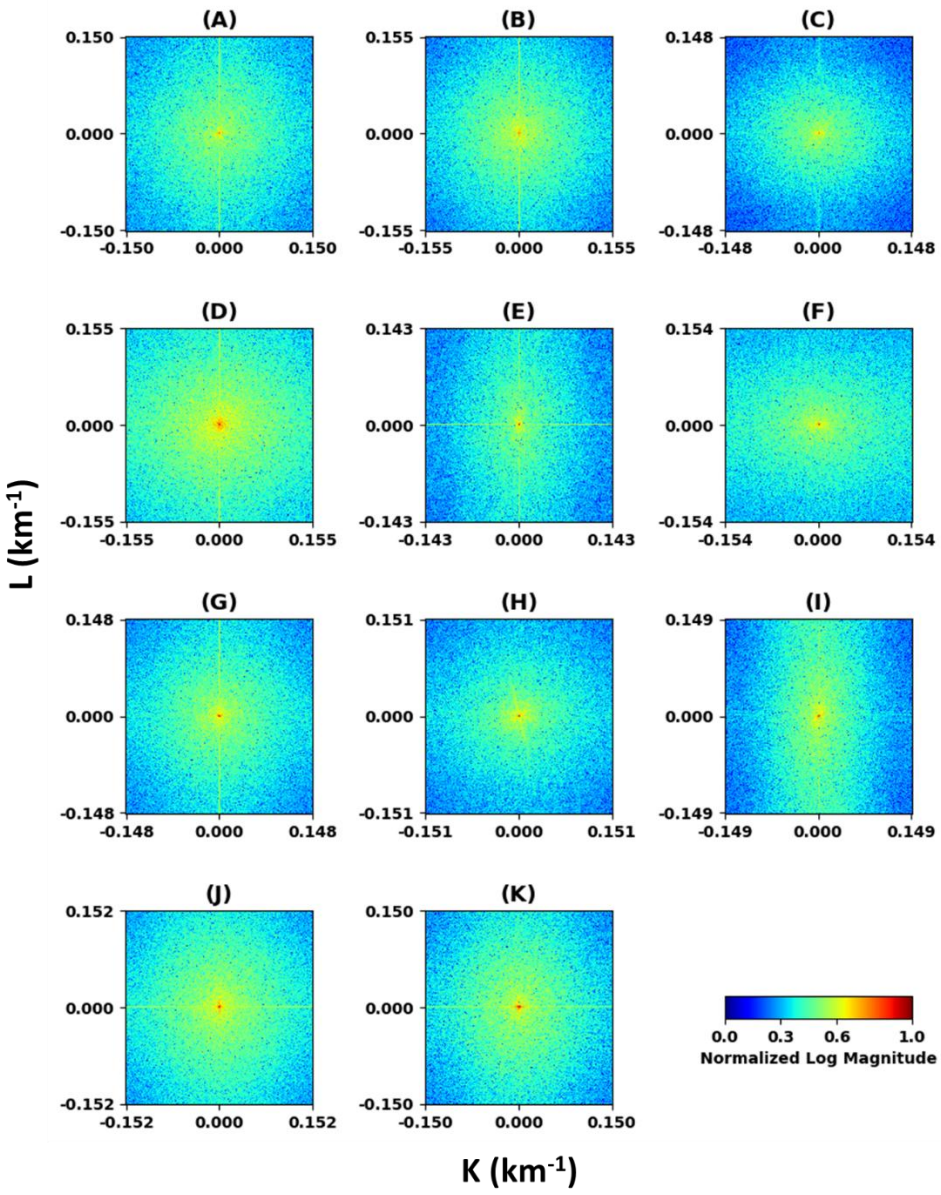

Figure 6. Fourier domain representation of height maps for selected Indian cities: (A) Ahmedabad, (B) Bangalore, (C) Chandigarh, (D) Chennai, (E) Delhi, (F) Hyderabad, (G) Jaipur, (H) Kolkata, (I) Mumbai, (J) Pune, and (K) Surat.

3.3 Variability Index of Building Height and Footprint in Indian Cities

Next, using the wavenumber domain representations of the building footprint and height shown in the previous section, an autocorrelation with an increasing shift distance was evaluated. The variations in the correlation coefficient with the shift distance for the footprint maps of the cities are shown in Fig. 7. For both 2018 and 2023, the correlation values demonstrate a monotonic linear decrease with the distance. A linear regression between the correlation coefficient and shift distance showed a coefficient of determination (R^2) greater than 0.8 for all cities, indicating a good linear fit.

From the linear regression models, the variability index could be obtained as the slope of the fitted lines (in Fig. 7 and Fig. 8). The variability index represents the rate of spatial change of building morphology in any city, where a high variability index means higher non-uniformity as the correlation breaks down rapidly with the shift distance. For the variations in footprint shown in Fig. 7, the variability index varies between 0.0351 km^{-1} and 0.0557 km^{-1} for all cities in 2023, with Chandigarh having the highest variability index and Mumbai having the lowest. In terms of decreasing variability of footprint in 2023, the Indian cities can be arranged in the following order: Chandigarh, Pune, Bangalore, Chennai, Hyderabad, Jaipur, Surat, Ahmedabad, Kolkata, Delhi, and Mumbai. This trend of changing variability also indicates the degree of planning in an urban area and the patterns in the shape and size of the buildings. For example, with the lowest footprint variability, Mumbai has buildings of a similar area spread all over the city. This is anecdotally confirmed by the dense habitations that Mumbai is known for.

Moreover, the divergence between the fitted lines of 2018 and 2023 demonstrates the effect of the recent construction activities. In the older industrial and commercial hubs such as Ahmedabad, Delhi, Kolkata, Mumbai, Pune, and Surat, where the cities have not changed significantly over that time, the variability index does not show a significant change between 2018 and 2023. On the contrary, cities like Chennai, Hyderabad, and Jaipur demonstrated a higher change in footprint variability. Moreover, on average, the correlation completely breaks down after ~9 km, indicating that the building footprints are completely random outside this shift distance. Similar inferences on height variability can also be drawn from observing the variability index of cities in Fig. 8. For example, the correlation coefficient for building heights also breaks down after ~9 km, where the variability index of height lies between 0.0441 km^{-1} and 0.0739 km^{-1} for all cities. The highest variability in height is observed for Bangalore, and the lowest is for Mumbai. Moreover, in terms of decreasing height variability in 2023, the Indian cities can be arranged in the following order: Bangalore, Pune, Chandigarh, Surat, Chennai, Jaipur, Kolkata, Ahmedabad, Hyderabad, Delhi, and Mumbai. The trends in height and footprint variability

indicate that Delhi and Mumbai have the lowest variabilities, which could be due to the dense urban clusters in these cities, where the building morphology does not change much. The temporal changes in the variability index are discussed in the next section, along with the comparison between height and footprint variability.

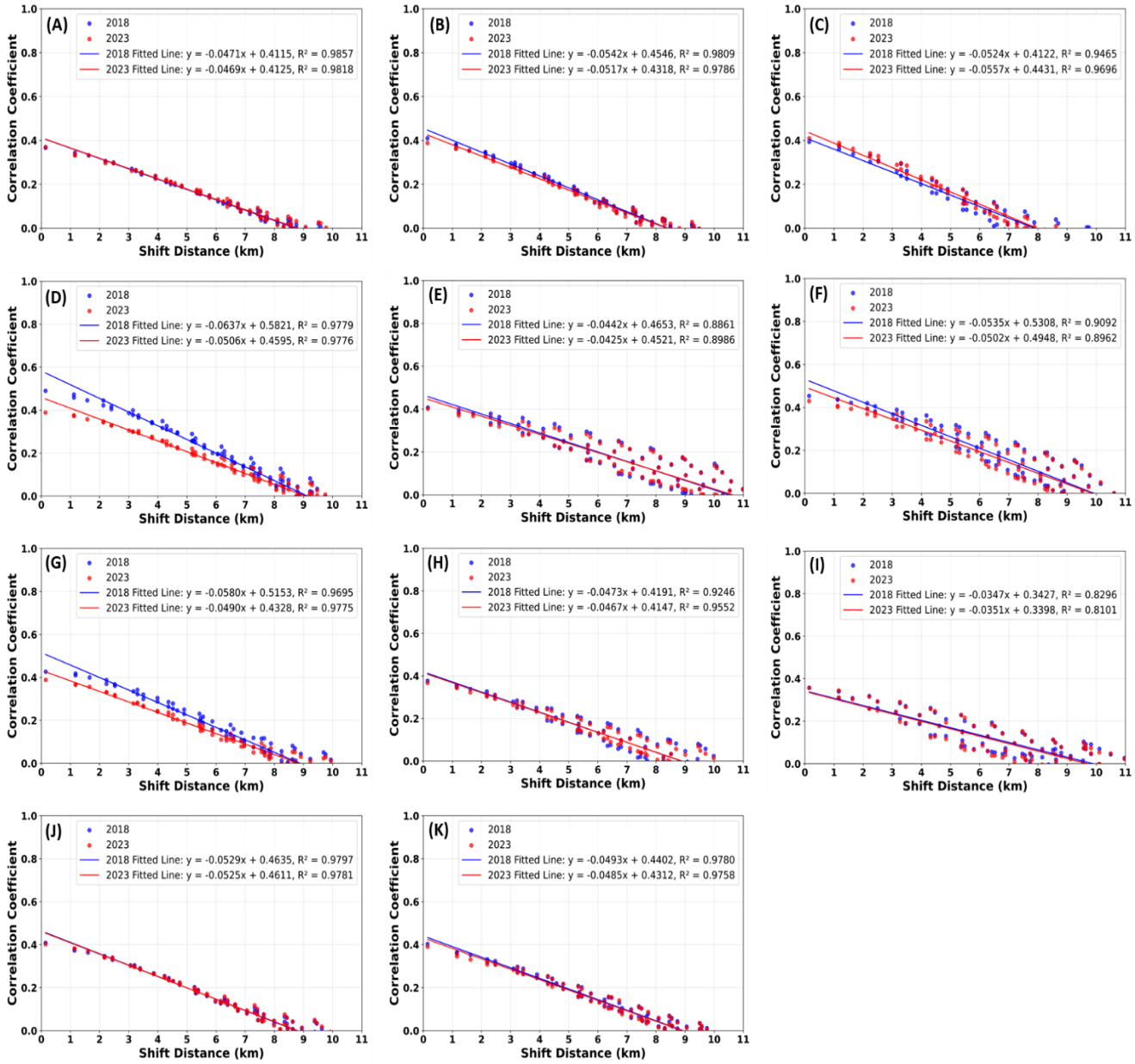

Figure 7. Correlation Coefficient Variations with Ground Distance Shifted in Footprint Maps for (A) Ahmedabad, (B) Bangalore, (C) Chandigarh, (D) Chennai, (E) Delhi, (F) Hyderabad, (G) Jaipur, (H) Kolkata, (I) Mumbai, (J) Pune, and (K) Surat.

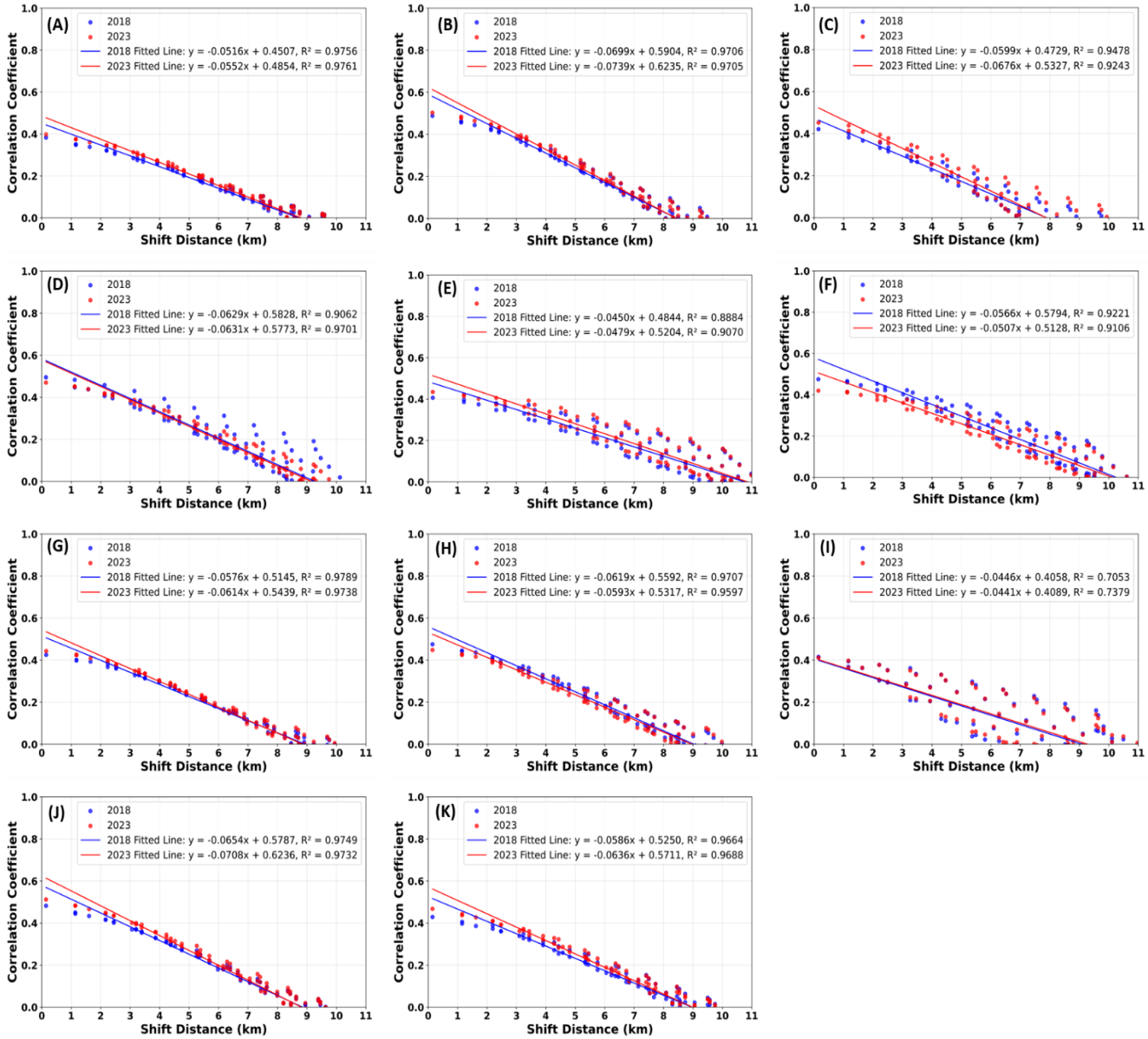

Figure 8. Correlation Coefficient Variations with Ground Distance Shifted in Height Maps for (A) Ahmedabad, (B) Bangalore, (C) Chandigarh, (D) Chennai, (E) Delhi, (F) Hyderabad, (G) Jaipur, (H) Kolkata, (I) Mumbai, (J) Pune, and (K) Surat.

3.4 Temporal Changes in Variability Index

A comparative analysis of the variability index of building footprint and height between 2018 and 2023 is shown in Fig. 9, where the arrow points from 2018 to 2023. The direction of the arrow denotes the sign of the change, and the length of the arrow is the magnitude of the change. Barring a single instance of increasing footprint variability for Chandigarh, the building footprint variability index either remained similar or decreased for all 11 Indian cities from 2018 to 2023. This trend could be due to two reasons: (a) the recently constructed buildings have a similar footprint as the existing building

stock, and/or (b) the total building stock has not changed compared to 2018. Contrarily, the height variability (Fig. 9B) has increased or remained the same for most cities except for Hyderabad and Kolkata, where a decreasing trend has been observed. The combination of footprint and height variability indicates that the individual buildings' footprint has remained almost constant, while the height of the buildings has altered (mostly increased) between 2018 and 2023.

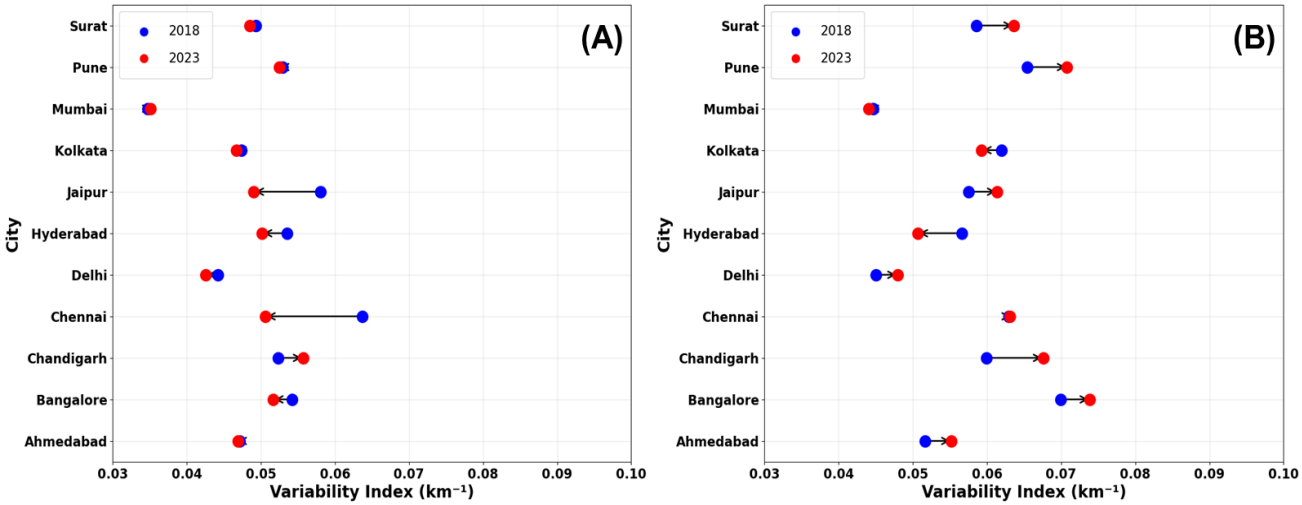

Figure 9. Variability index in (A) footprint and (B) height of different Indian cities for 2018 and 2023. The direction of the arrow indicates the movement from 2018 to 2023, and its length represents the magnitude of change.

Furthermore, a comparison between the footprint and height variability is shown in Fig. 10A. The 45-degree line indicates the same rate of change in footprint and height, and any deviation from there suggests that the footprint and height change with different variability. The best-fit line for 2018 and 2023 (Fig. 10A) indicates that the height variability exceeds the footprint variability. However, in 2018, a few cities (Chennai, Delhi, and Jaipur) had the same height and footprint variability. From 2018 to 2023, the best-fit line shifted downwards towards the height variability, indicating that the height variability further increased compared to the footprint variability for most of the cities, except Hyderabad, which moved towards the 45-degree line, and Mumbai, which remained almost the same. Moreover, an overall variability index (Fig. 10B) has been estimated for all cities, calculated as the root mean square of the height and footprint variability. Based on the overall variability, the cities in the descending order of variability have been ranked as follows for 2023: Bangalore, Pune, Chandigarh, Chennai, Surat, Jaipur, Kolkata, Ahmedabad, Hyderabad, Delhi, and Mumbai. The most significant

change in variability from 2018 to 2023 has been observed in Chennai, followed by Chandigarh and Hyderabad.

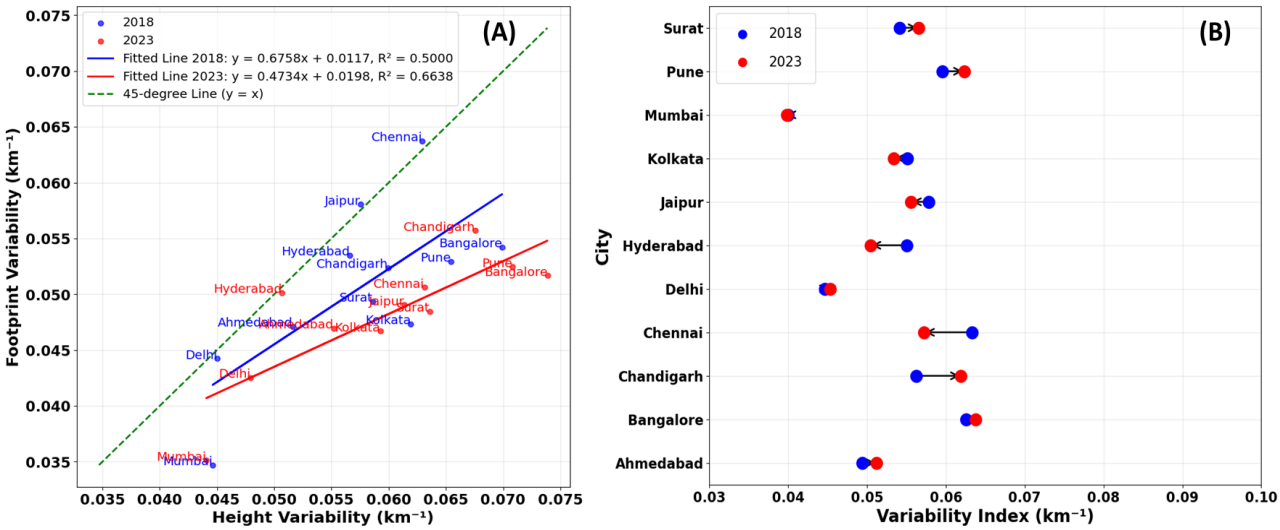

Figure 10. (A) Footprint vs. height and (B) overall variability index for Indian cities.

4. Conclusion

Owing to the impact buildings have on the environment, economy, and societal development, it is imperative to study the building morphology in developing countries like India. This work developed a novel framework to examine the variability of building footprint and height in major Indian cities. A pre-trained deep learning model named SHAFTS has been used to obtain the maps of building features based on remote sensing data. These maps have been further processed to identify patterns and analyze the spatial and temporal variations in the building structures.

The investigation carried out in this work indicates the non-homogeneity in building morphology of Indian cities, where the average variability indices in footprint and height are 0.0481 and 0.0598, respectively, for 2023. Compared to 2018, the variability in height has increased by ~4%, and the variability in footprint has decreased by ~5% in 2023. These patterns in variability suggest that the building footprint, on average, has remained constant, i.e., the new buildings have the same footprint as the older ones, thereby reducing the variability in the footprint. Contrarily, the increased height variability indicates different heights of older buildings compared to newly constructed buildings. The analysis conducted in this work also shows that the variability in height is ~24% more than the

footprint. This difference in height and footprint variability could be due to space constraints that limit the horizontal expansion of buildings, with buildings growing vertically instead to accommodate the substantial increase in urban population and subsequent housing demand. The combined variability has no definite temporal trend, with some cities demonstrating increased overall variability (Chandigarh, Pune, and Surat), some with decreased variability (Chennai, Hyderabad, and Jaipur), and many cities with minor to no changes in the variability (Ahmedabad, Bangalore, Delhi, Kolkata, and Mumbai). This heterogeneity illustrates the generally unplanned nature of urban expansion in these Indian cities.

This work examined the spatial and temporal disparity of building morphology in Indian cities at a coarse resolution of ~100 m and utilized a pre-trained and pre-validated deep-learning model. It is inherently considered that the model can be generalised, which might introduce some deviations relative to the ground truth. However, without a substantial ground truth measurement, the framework developed in this study and similar deep learning models can provide crucial insights into urban morphology in Indian cities.

Acknowledgments

Nishchaya Mishra's funding for this work was provided by IIT Gandhinagar. The authors thank Mr. Hiren Solanki for his initial assistance with the SHAFTS model.

Statements and Declarations

The authors declare that they have no known competing financial interests or personal relationships that could potentially influence the reported work.

References

[1] Urban Development Overview n.d. https://www.worldbank.org/en/topic/urbandevelopment/overview (accessed January 1, 2025).

[2] Duranton G, Puga D. The Growth of Cities. Handbook of Economic Growth 2014;2:781–853. https://doi.org/10.1016/B978-0-444-53540-5.00005-7.

[3] Global Status Report for Buildings and Construction | UNEP - UN Environment Programme n.d. https://www.unep.org/resources/report/global-status-report-buildings-and-construction (accessed January 1, 2025).

[4] Buildings - Energy System - IEA n.d. https://www.iea.org/energy-system/buildings (accessed January 1, 2025).

[5] Mishra NK, Patel S. Need for a Holistic Approach to Assessing Sustainable, Green, and Healthy Buildings. Environment & Health 2024. https://doi.org/10.1021/ENVHEALTH.4C00161.

[6] Mirasgedis S, Cabeza LF, Vérez D. Contribution of buildings climate change mitigation options to sustainable development. Sustain Cities Soc 2024;106:105355. https://doi.org/10.1016/J.SCS.2024.105355.

[7] Mishra NK, Vance ME, Novoselac A, Patel S. Dynamic optimization of personal exposure and energy consumption while ensuring thermal comfort in a test house. Build Environ 2024;252:111265. https://doi.org/10.1016/J.BUILDENV.2024.111265.

[8] Faulkner CA, Castellini JE, Lou Y, Zuo W, Lorenzetti DM, Sohn MD. Tradeoffs among indoor air quality, financial costs, and CO2 emissions for HVAC operation strategies to mitigate indoor virus in U.S. office buildings. Build Environ 2022;221:109282. https://doi.org/10.1016/J.BUILDENV.2022.109282.

[9] Mishra NK, Batra N, Patel S. Optimizing Pollutant Exposure, Energy Consumption, and Thermal Comfort in a House via Deep Reinforcement Learning Control. Journal of Building Engineering 2025:114074. https://doi.org/10.1016/J.JOBE.2025.114074.

[10] Che Y, Li X, Liu X, Xu X, Huang K, Zhu P, et al. Mapping of individual building heights reveals the large gap of urban-rural living spaces in the contiguous US. The Innovation Geoscience 2024;2:100069–1. https://doi.org/10.59717/J.XINN-GEO.2024.100069.

[11] Ali HH, Al-Betawi YN, Al-Qudah HS. Effects of urban form on social sustainability – A case study of Irbid, Jordan. International Journal of Urban Sustainable Development 2019;11:203–22. https://doi.org/10.1080/19463138.2019.1590367.

[12] Bolte AM, Kistemann T, Dehbi Y, Kötter T. (Un)just Distribution of Visible Green Spaces? A Socio-Economic Window View Analysis on Residential Buildings: The City of Cologne as Case Study. Journal of Geovisualization and Spatial Analysis 2025;9:1–24. https://doi.org/10.1007/S41651-025-00214-7/FIGURES/5.

[13] Bonsu K, Bonin O. Urban Growth Process in Greater Accra Metropolitan Area: Characterization Using Fractal Analysis. Journal of Geovisualization and Spatial Analysis 2023;7:1–19. https://doi.org/10.1007/S41651-023-00149-X/TABLES/11.

[14] Yang L, Chen Y, Li Y, Zhu H, Yang X, Li S, et al. Is 3D building morphology really related to land surface temperature? Insights from a new homogeneous unit. Build Environ 2024;266:112101. https://doi.org/10.1016/J.BUILDENV.2024.112101.

[15] Qiao Z, Han X, Wu C, Liu L, Xu X, Sun Z, et al. Scale Effects of the Relationships between 3D Building Morphology and Urban Heat Island: A Case Study of Provincial Capital Cities of Mainland China. Complexity 2020;2020:9326793. https://doi.org/10.1155/2020/9326793.

[16] Liang Z, Wu S, Wang Y, Wei F, Huang J, Shen J, et al. The relationship between urban form and heat island intensity along the urban development gradients. Science of The Total Environment 2020;708:135011. https://doi.org/10.1016/J.SCITOTENV.2019.135011.

[17] Yang J, Shi Q, Menenti M, Wong MS, Wu Z, Zhao Q, et al. Observing the impact of urban morphology and building geometry on thermal environment by high spatial resolution thermal images. Urban Clim 2021;39:100937. https://doi.org/10.1016/J.UCLIM.2021.100937.

[18] Hoisington AJ, Stearns-Yoder KA, Schuldt SJ, Beemer CJ, Maestre JP, Kinney KA, et al. Ten questions concerning the built environment and mental health. Build Environ 2019;155:58–69. https://doi.org/10.1016/J.BUILDENV.2019.03.036.

[19] Fathi S, Sajadzadeh H, Sheshkal FM, Aram F, Pinter G, Felde I, et al. The Role of Urban Morphology Design on Enhancing Physical Activity and Public Health. International Journal of Environmental Research and Public Health 2020, Vol 17, Page 2359 2020;17:2359. https://doi.org/10.3390/IJERPH17072359.

[20] Wang Y, Sun G, Wu Y, Rosenberg MW. Urban 3D building morphology and energy consumption: empirical evidence from 53 cities in China. Scientific Reports 2024 14:1 2024;14:1–13. https://doi.org/10.1038/s41598-024-63698-1.

[21] Shareef S, Altan H. Urban block configuration and the impact on energy consumption: A case study of sinuous morphology. Renewable and Sustainable Energy Reviews 2022;163:112507. https://doi.org/10.1016/J.RSER.2022.112507.

[22] Javanroodi K, Mahdavinejad M, Nik VM. Impacts of urban morphology on reducing cooling load and increasing ventilation potential in hot-arid climate. Appl Energy 2018;231:714–46. https://doi.org/10.1016/J.APENERGY.2018.09.116.

[23] Hassan AM, ELMokadem AA, Megahed NA, Abo Eleinen OM. Urban morphology as a passive strategy in promoting outdoor air quality. Journal of Building Engineering 2020;29:101204. https://doi.org/10.1016/J.JOBE.2020.101204.

[24] Hassan AM, Fatah El Mokadem AA, Megahed NA, Abo Eleinen OM. Improving outdoor air quality based on building morphology: Numerical investigation. Frontiers of Architectural Research 2020;9:319–34. https://doi.org/10.1016/J.FOAR.2020.01.001.

[25] Liang L, Gong P. Urban and air pollution: a multi-city study of long-term effects of urban landscape patterns on air quality trends. Scientific Reports 2020 10:1 2020;10:1–13. https://doi.org/10.1038/s41598-020-74524-9.

[26] Hong S, Wang C, Wang W, Zhang P, Guo Y, Ma Z, et al. Urban 2D and 3D morphology and the pattern of ozone pollution: a 68-city study in China. Landsc Ecol 2024;39:1–22. https://doi.org/10.1007/S10980-024-01838-8/FIGURES/12.

[27] Li SY, Han JY. The impact of shadow covering on the rooftop solar photovoltaic system for evaluating self-sufficiency rate in the concept of nearly zero energy building. Sustain Cities Soc 2022;80:103821. https://doi.org/10.1016/J.SCS.2022.103821.

[28] Wang Q, Peng LLH, Jiang W, Yin S, Feng N, Yao L. Urban form affects the cool island effect of urban greenery via building shadows. Build Environ 2024;254:111398. https://doi.org/10.1016/J.BUILDENV.2024.111398.

[29] Zou Y, Chen J, Zong H. Is shading a better way to cool down? Evaluation and comparison of the cooling capacity of blue-green spaces and urban shade. Ecol Indic 2024;167:112688. https://doi.org/10.1016/J.ECOLIND.2024.112688.

[30] Li R, Sun T, Tian F, Ni GH. SHAFTS (v2022.3): A deep-learning-based Python package for simultaneous extraction of building height and footprint from sentinel imagery. Geosci Model Dev 2023;16:751–78. https://doi.org/10.5194/gmd-16-751-2023.

[31] Stipek C, Hauser T, Adams D, Epting J, Brelsford C, Moehl J, et al. Inferring building height from footprint morphology data. Scientific Reports 2024 14:1 2024;14:1–14. https://doi.org/10.1038/s41598-024-66467-2.

[32] Alqurashi AF, Kumar L. Spatiotemporal patterns of urban change and associated environmental impacts in five Saudi Arabian cities: A case study using remote sensing data. Habitat Int 2016;58:75–88. https://doi.org/10.1016/J.HABITATINT.2016.10.001.

[33] Verma D, Jana A, Ramamritham K. Transfer learning approach to map urban slums using high and medium resolution satellite imagery. Habitat Int 2019;88:101981. https://doi.org/10.1016/J.HABITATINT.2019.04.008.

[34] Bonczak B, Kontokosta CE. Large-scale parameterization of 3D building morphology in complex urban landscapes using aerial LiDAR and city administrative data. Comput Environ Urban Syst 2019;73:126–42. https://doi.org/10.1016/J.COMPENVURBSYS.2018.09.004.

[35] Wu C, Wang J, Wang M, Kraak MJ. Machine learning-based characterisation of urban morphology with the street pattern. Comput Environ Urban Syst 2024;109:102078. https://doi.org/10.1016/J.COMPENVURBSYS.2024.102078.

[36] Luo L, Li P, Yan X. Deep Learning-Based Building Extraction from Remote Sensing Images: A Comprehensive Review. Energies 2021, Vol 14, Page 7982 2021;14:7982. https://doi.org/10.3390/EN14237982.

[37] Frantz D, Schug F, Okujeni A, Navacchi C, Wagner W, van der Linden S, et al. National-scale mapping of building height using Sentinel-1 and Sentinel-2 time series. Remote Sens Environ 2021;252:112128. https://doi.org/10.1016/J.RSE.2020.112128.

[38] Mallick SK, Rudra S, Maity B. Unplanned urban built-up growth creates problem in human adaptability: Evidence from a growing up city in eastern Himalayan foothills. Applied Geography 2023;150:102842. https://doi.org/10.1016/J.APGEOG.2022.102842.

[39] Global Construction Futures | Oxford Economics n.d. https://www.oxfordeconomics.com/resource/global-construction-futures/?utm_source=economicuncertainty&utm_medium=blog&utm_campaign=construction&utm_content=recent_release&utm_term=7018e00000093KzAAI (accessed January 1, 2025).

[40] Anjomshoaa A, Kondor D, Helfert M, Amini S, Saber M, Rabiei-Dastjerdi H, et al. Urban Land Use and Land Cover Change Analysis Using Random Forest Classification of Landsat Time Series. Remote Sensing 2022, Vol 14, Page 2654 2022;14:2654. https://doi.org/10.3390/RS14112654.

[41] Hossain MS, Khan MAH, Oluwajuwon TV, Biswas J, Rubaiot Abdullah SM, Tanvir MSSI, et al. Spatiotemporal change detection of land use land cover (LULC) in Fashiakhali wildlife

sanctuary (FKWS) impact area, Bangladesh, employing multispectral images and GIS. Model Earth Syst Environ 2023;9:3151–73. https://doi.org/10.1007/S40808-022-01653-7/FIGURES/5.

[42] Seyam MMH, Haque MR, Rahman MM. Identifying the land use land cover (LULC) changes using remote sensing and GIS approach: A case study at Bhaluka in Mymensingh, Bangladesh. Case Studies in Chemical and Environmental Engineering 2023;7:100293. https://doi.org/10.1016/J.CSCEE.2022.100293.

[43] Patel A, Vyas D, Chaudhari N, Patel R, Patel K, Mehta D. Novel approach for the LULC change detection using GIS & Google Earth Engine through spatiotemporal analysis to evaluate the urbanization growth of Ahmedabad city. Results in Engineering 2024;21:101788. https://doi.org/10.1016/J.RINENG.2024.101788.

[44] Cheng G, Huang Y, Li X, Lyu S, Xu Z, Zhao H, et al. Change Detection Methods for Remote Sensing in the Last Decade: A Comprehensive Review. Remote Sensing 2024, Vol 16, Page 2355 2024;16:2355. https://doi.org/10.3390/RS16132355.

[45] Inkoom JN, Nyarko BK, Antwi KB. Explicit Modeling of Spatial Growth Patterns in Shama, Ghana: an Agent-Based Approach. Journal of Geovisualization and Spatial Analysis 2017;1:1–21. https://doi.org/10.1007/S41651-017-0006-2/FIGURES/15.

[46] Sikder SK, Behnisch M, Herold H, Koetter T. Geospatial Analysis of Building Structures in Megacity Dhaka: the Use of Spatial Statistics for Promoting Data-driven Decision-making. Journal of Geovisualization and Spatial Analysis 2019;3:1–14. https://doi.org/10.1007/S41651-019-0029-Y/FIGURES/9.

[47] Google Earth Engine n.d. https://earthengine.google.com/ (accessed July 18, 2025).

[48] GitHub - LlIC-mmd/SHAFTS: simultaneous extraction of building height and footprint n.d. https://github.com/LlIC-mmd/SHAFTS?tab=readme-ov-file (accessed January 1, 2025).

[49] Cooley JW, Tukey JW. An algorithm for the machine calculation of complex Fourier series. Math Comput 1965;19:297–301. https://doi.org/10.1090/S0025-5718-1965-0178586-1.

[50] Image Transforms - Fourier Transform n.d. https://homepages.inf.ed.ac.uk/rbf/HIPR2/fourier.htm (accessed January 1, 2025).

[51] John AM, Khanna K, Prasad RR, Pillai LG. A review on application of fourier transform in image restoration. Proceedings of the 4th International Conference on IoT in Social, Mobile, Analytics and Cloud, ISMAC 2020 2020:389–97. https://doi.org/10.1109/I-SMAC49090.2020.9243510.